Investigation of Linear and Damage-Coupled Viscoelastic Properties of Sustainable Asphalt Mixture Using a Micromechanical Finite Element Approach

Qingli Dai [1] and Zhanping You [2]

Abstract

This paper presents a microstructure-based finite element model by incorporating elastic aggregates and viscoelastic sand mastic. The microstructure-based finite element (FE) approach was used to predict the linear and damage-coupled viscoelastic properties of reclaimed asphalt mixture. The two-dimensional (2D) microstructure of asphalt mixture was obtained from the scanned image of a smoothly sawn surface of a reclaimed asphalt pavement (RAP) mixture specimen. In the microstructure, the sketches of highly irregular aggregates were converted into polygons. The whole microstructure model was divided into highly irregular aggregate and sand mastic subdomains. The finite element mesh was generated within each subdomain. The deformation of the aggregate and mastic subdomains was connected through the sharing boundary nodes. Linear and damage-coupled viscoelastic finite element model was developed with displacement-based incremental formulation. The linear and damage-coupled viscoelastic simulation was conducted on the image sample of test specimen under different sinusoidal force loading frequencies. The uniaxial compression simulation results showed creep deformation constant cyclic force loading amplitude and damage-coupled viscoelastic responses have larger creep deformation. Simulations under different loading frequencies found compression strain deceases with loading frequencies due to less relaxation time.

Introduction

A sustainable asphalt mixture is designed to consider the economic, societal, and environmental factors through life cycle analysis. The use of reclaimed asphalt pavement (RAP) material has been considered as sustainable asphalt mixtures and has obtained varying degrees of success in the United States. The asphalt pavement recycling methods include hot mix recycling, hot in-place recycling, cold in-place recycling and full depth reclamation. Hot mix recycling is the predominant method of structural recycling and the mix design procedure is basically similar as the one for new mixtures with the additional requirement for asphalt pavement analysis (Roberts et al. 1996). A recycled mixture should be designed to produce an asphalt material having the same properties as that in a new one. The aged asphalt binder must be mixed with the new asphalt binder or recycling agent to provide the overall desired binder properties. Recent study have reported

[1] Visiting Assistant Professor, School of Technology and Department of Mechanical Engineering-Engineering Mechanics, Michigan Technological University, Houghton, 1400 Townsend Drive, MI 49931. qingdai@mtu.edu

[2] Tomasini Assistant Professor, Dept. of Civil and Environmental Engineering, Michigan Technological University, 1400 Townsend Drive, Houghton, MI 49931. zyou@mtu.edu

investigations of the performance of Superpave asphalt mixtures incorporating RAP (McDaniel and Shah 2003) and mechanical properties of RAP (Picado-Santos et al. 2004). However, there still exists uncertainty on proper recycling processes and on the subsequent performance of the recycled product.

Asphalt mixture is a composite material of graded aggregates bound with mastic (asphalt binder plus fine aggregates and fines). Recycling processes further complicate the mechanical behavior by introducing additional variation of these constituents, and by adding several ageing/time-dependent effects. For such materials, the macro properties depend on many micro phenomena that occur at the aggregate/mastic level. A fundamental knowledge of the material behavior is needed to understand and explain recycling issues, and a micromechanical model would be an excellent tool to establish such basic mechanisms.

Asphalt mixture were investigated by non-interaction particle micromechanics models without specified geometry (Buttlar and Roque 1996; Buttlar and Roque 1997; Hashin and Shtrikman 1963; Schapery 1969; Voigt 1889), as well as, with specified geometry (Buttlar et al. 1999; Christensen and Lo 1979; Hashin 1965; Shashidhar et al. 1996). A two-dimensional (2D) micro-fabric discrete element model (MDEM) concept was developed and calibrated to predict the stiffness of asphalt mixtures (You and Buttlar 2004; You and Buttlar 2005; You and Buttlar 2006).

Finite element modeling of asphalt concrete microstructure potentially allows accurate modeling of aggregate and mastic complex constitutive behaviors and microstructure geometries. Research work has been conducted using finite element techniques (Bahia et al. 1999; Bazant 1990; Budhu et al. 1997; Guddati et al. 2002; Kose et al. 2000; Mora 1992; Mustoe and Griffiths 1998; Papagiannakis et al. 2002; Sepehr et al. 1994; Stankowski 1990). In addition, an equivalent lattice network approach was applied, where the local interaction between neighboring particles was modeled with a special frame-type finite element (Dai and Sadd 2004; Dai et al. 2005; Sadd et al. 2004b; Sadd et al. 2004c). A mixed finite element approach was developed to study asphalt mixture by using continuum elements for the effective asphalt mastic and rigid body defined with rigid elements for each aggregate (Dai et al. 2006). A unified approach for the rate-independent and rate-dependent damage behavior has been developed using Schapery's nonlinear viscoelastic model. Properties of the continuum elements are specified through a user material subroutine within the ABAQUS code and this allows linear and damage-coupled viscoelastic constitutive behavior of the mastic cement to be incorporated. In these models, the microstructure of real asphalt materials is simulated with idealized elliptical aggregate and rectangular effective mastic zone (Dai 2004). Using image processing and ellipse fitting methods, particle dimensions and locations were determined from digital photographs of the sample's surface microstructure. The objectives of this study are 1) develop a microstructure-based finite element model by incorporating elastic aggregates with viscoelastic sand mastic 2) numerically investigate the linear and damage-coupled viscoelastic behavior of reclaimed asphalt mixture.

Microstructure of asphalt mixture

In this study, the two-dimensional (2D) microstructure of asphalt mixture was obtained by optically scanning smoothly sawn asphalt mixture test specimens. A high-resolution scanner was used to obtain grayscale images from the sections (You and

Buttlar 2006). Image processing technique was used to converted the image into many-sided polygons using a custom developed macro program to define the microstructure of asphalt mixture (Buttlar and You 2001). The average of the polygon diameter was chosen as a threshold to determine which aggregates would be "retained" on a given sieve (the rest of the aggregates would be "passed" the given sieve), although some other measurement parameters were also attempted in analyzing the gradation of the aggregates (You 2003). The polygons used in the micromechanical model were filtered as coarse aggregates. In the model of the asphalt mixture, the coarse aggregates retained on 2.36mm sieve (No. 8) were counted in the subdomain of aggregate. The fine aggregates passing 2.36mm were filtered as sand mastic. Elastic properties of aggregates were measured and applied to aggregate subdomain, and viscoelastic mastic properties were also calibrated with mastic creep tests (Dai and You 2007). Finite element simulation was conducted to predict the global mixture behavior by combining aggregate and mastic properties.

FE Incremental Formulation for Linear Viscoelastic Behavior

The linear constitutive behavior for this Maxwell-type model can be expressed as a hereditary integral

$$\sigma_{ij} = E_{\infty}\varepsilon_{ij} + \int_0^t E_t \frac{d\varepsilon_{ij}(\tau)}{d\tau} d\tau, \tag{1}$$

where E_t is the transient modulus changing with time, and expressed with a Prony series

$$E_t = \sum_{m=1}^{M} E_m e^{-\frac{(t-\tau)}{\rho_m}}, \text{ and } \rho_m = \frac{\eta_m}{E_m} \tag{2}$$

In these equations, E_m, η_m and ρ_m are the spring constant, dashpot viscosity and relaxation time respectively for the m^{th} Maxwell element.

The reduced time (effective time) is defined by using time-temperature superposition principle as

$$\xi(t) = \int_0^t \frac{1}{\alpha_T} d\tau \tag{3}$$

where the term $\alpha_T = \alpha_T(T(\tau))$ is a temperature-dependent time-scale shift factor.

Three-dimensional behavior can be formulated with uncoupled volumetric and deviatoric stress-strain relations. A displacement-based incremental finite element modeling scheme with constant strain rate over each increment was developed in the following format:

$$\Delta\sigma = K \cdot \Delta\varepsilon + \Delta\sigma^R \tag{4}$$

Where $\Delta\sigma$ and $\Delta\varepsilon$ are incremental stress and strain, K is the incremental stiffness and $\Delta\sigma^R$ is the residue stress vector.

The incremental formulation of the volumetric behavior is obtained with constant volumetric strain rate $R_{kk} = \frac{\Delta\varepsilon_{kk}}{\Delta\xi}$,

$$\Delta\sigma_{kk} = 3\left[K_{\infty} + \sum_{m=1}^{N} \frac{K_m \rho_m}{\Delta\xi}\left(1 - e^{-\frac{\Delta\xi}{\rho_m}}\right)\right]\Delta\varepsilon_{kk} + \Delta\sigma_{kk}^R \tag{5}$$

where K_∞ and K_m are bulk moduli, and the residual part $\Delta\sigma_{kk}^R$ can be expressed in a recursive relation with the history variable S_m,

$$\Delta\sigma_{kk}^R = \sum_{m=1}^{M} -\left(1-e^{-\frac{\Delta\xi}{\rho_m}}\right)S_m(\xi_n), \text{ and } S_m(\xi_n) = 3K_m R_{kk}\rho_m\left(1-e^{-\frac{\Delta\xi}{\rho_m}}\right) + S_m(\xi_{n-1})e^{-\frac{\Delta\xi}{\rho_m}} \quad (6)$$

For the initial increment, the history variable $S_m(\xi_1)$ equals to $3K_m R_{kk}\rho_m\left(1-e^{-\frac{\Delta\xi}{\rho_m}}\right)$ and is similar to the following formulations.

The formulation of the deviatoric behavior with deviatoric stress $\hat{\sigma}_{ij} = \sigma_{ij} - \frac{1}{3}\sigma_{kk}\delta_{ij}$ and strain $\hat{\varepsilon}_{ij} = \varepsilon_{ij} - \frac{1}{3}\varepsilon_{kk}\delta_{ij}$ is obtained with constant deviatoric strain rate $\hat{R}_{ij} = \frac{\Delta\hat{\varepsilon}_{ij}}{\Delta\xi}$,

$$\Delta\hat{\sigma}_{ij} = 2\left[G_\infty + \sum_{m=1}^{N}\frac{G_m\rho_m}{\Delta\xi}\left(1-e^{-\frac{\Delta\xi}{\rho_m}}\right)\right]\Delta\hat{\varepsilon}_{ij} + \Delta\hat{\sigma}_{ij}^R \quad (7)$$

and the residual part $\Delta\hat{\sigma}_{ij}^R$ can be expressed in the recursive relation

$$\Delta\hat{\sigma}_{ij}^R = \sum_{m=1}^{N} -\left(1-e^{-\frac{\Delta\xi}{\rho_m}}\right)S_m(\xi_n), \text{ and } S_m(\xi_n) = 2G_m\hat{R}_{ij}\rho_m\left(1-e^{-\frac{\Delta\xi}{\rho_m}}\right) + S_m(\xi_{n-1})e^{-\frac{\Delta\xi}{\rho_m}} \quad (8)$$

Normal incremental stresses can be formulated with combination of volumetric and deviatoric behaviors, while shear incremental stresses can be obtained from deviatoric behaviors. Once the incremental stress components are developed, the incremental stiffness terms can be calculated and then the incremental 3D linear viscoelastic behavior was formulated as

$$\begin{bmatrix}\Delta\sigma_{xx}\\ \Delta\sigma_{yy}\\ \Delta\sigma_{zz}\\ \Delta\sigma_{xy}\\ \Delta\sigma_{yz}\\ \Delta\sigma_{xz}\end{bmatrix} = \begin{bmatrix} K_1 & K_2 & K_2 & 0 & 0 & 0\\ \cdot & K_1 & K_2 & 0 & 0 & 0\\ \cdot & \cdot & K_1 & 0 & 0 & 0\\ \cdot & \cdot & \cdot & K_3 & 0 & 0\\ \cdot & \cdot & \cdot & \cdot & K_3 & 0\\ \cdot & \cdot & \cdot & \cdot & \cdot & K_3\end{bmatrix}\begin{bmatrix}\Delta\varepsilon_{xx}\\ \Delta\varepsilon_{yy}\\ \Delta\varepsilon_{zz}\\ \Delta\varepsilon_{xy}\\ \Delta\varepsilon_{yz}\\ \Delta\varepsilon_{xz}\end{bmatrix} + \begin{bmatrix}\Delta\sigma_{kk}^R + \Delta\hat{\sigma}_{xx}^R\\ \Delta\sigma_{kk}^R + \Delta\hat{\sigma}_{yy}^R\\ \Delta\sigma_{kk}^R + \Delta\hat{\sigma}_{zz}^R\\ \Delta\hat{\sigma}_{xy}^R\\ \Delta\hat{\sigma}_{yz}^R\\ \Delta\hat{\sigma}_{zx}^R\end{bmatrix} \quad (9)$$

where

$$\begin{aligned} K_1 &= \left[K_\infty + \sum_{m=1}^{N}\frac{K_m\rho_m}{\Delta\xi}\left(1-e^{-\frac{\Delta\xi}{\rho_m}}\right)\right] + \frac{4}{3}\left[G_\infty + \sum_{m=1}^{N}\frac{G_m\rho_m}{\Delta\xi}\left(1-e^{-\frac{\Delta\xi}{\rho_m}}\right)\right]\\ K_2 &= \left[K_\infty + \sum_{m=1}^{N}\frac{K_m\rho_m}{\Delta\xi}\left(1-e^{-\frac{\Delta\xi}{\rho_m}}\right)\right] - \frac{2}{3}\left[G_\infty + \sum_{m=1}^{N}\frac{G_m\rho_m}{\Delta\xi}\left(1-e^{-\frac{\Delta\xi}{\rho_m}}\right)\right]\\ K_3 &= 2\left[G_\infty + \sum_{m=1}^{N}\frac{G_m\rho_m}{\Delta\xi}\left(1-e^{-\frac{\Delta\xi}{\rho_m}}\right)\right] \end{aligned} \quad (10)$$

FE Incremental Formulation for Damage-Coupled Viscoelastic Behavior

Reclaimed asphalt mixture has damage-coupled viscoelastic behavior. The original Schapery nonlinear viscoelastic model (Schapery 1969) was given as

$$\sigma(\xi) = h_e E_\infty \varepsilon(\xi) + \int_0^\xi h_1 E_t(\xi - \xi') \frac{d(h_2 \varepsilon(\xi'))}{d\xi'} d\xi' \tag{11}$$

This model incorporates three different nonlinear parameters: h_e is the nonlinear factor of the relaxed elastic modulus E_∞, h_1 measures the nonlinearity effect in the transient modulus E_t, and h_2 accounts for the loading rate effect.

Following form (11), a rate-independent damage-coupled viscoelastic model is proposed by replacing two nonlinear parameters h_e and h_1 with damage variables which would be expressed with damage evolution functions (Assume h_2=1 to neglect rate-dependent damage behavior in this study).

$$\sigma(\xi) = h_e(\varepsilon_{\max}) E_\infty \varepsilon(\xi) + \int_0^\xi h_1(\varepsilon_{\max}) E_t(\xi - \xi') \frac{d(\varepsilon(\xi'))}{d\xi'} d\xi' \tag{12}$$

where h_e and h_1 are the elastic and viscoelastic damage variables for the rate-independent failure behavior. These variables are functions of the maximum strain $\varepsilon_{\max}$, which is defined as the maximum value over the past history up to the current time ξ,

$$\varepsilon_{\max} = \max(\varepsilon(\xi')),\ \xi' \in [0, \xi] \tag{13}$$

The elastic damage variable $h_e = 1 - \Omega$ measures the relaxed elastic stiffness reduction, and can be described by using the inelastic damage evolution law in Sadd et al.(Sadd et al. 2004a; Sadd et al. 2004b),

$$h_e(\varepsilon_{\max}) = e^{-b\frac{\varepsilon_{\max}}{\varepsilon_0}} \tag{14}$$

where the material parameters ε_0 and b are related to the softening strain and damage evolution rate respectively.

The viscoelastic variable h_1 measures the damage effect in the transient modulus, and is chosen with the following exponential form by (Simo and Ju 1987),

$$h_1(\varepsilon_{\max}) = \beta + (1-\beta)\frac{1 - e^{-\left(\frac{\varepsilon_{\max}}{\varepsilon_0}\right)}}{\varepsilon_{\max}/\varepsilon_0},\ \beta \in [0,1] \tag{15}$$

The variable h_1 will reduce from 1 to β as the maximum strain $\varepsilon_{\max}$ increases, and ε_0 is also the softening stain.

Following the previous formulation procedures, the incremental formulation of the volumetric behavior is obtained with constant volumetric strain rate $R_{kk} = \frac{\Delta\varepsilon_{kk}}{\Delta\xi}$,

$$\Delta\sigma_{kk} = 3\left[K_\infty h_e(\varepsilon^{kk}_{\max}) + \sum_{m=1}^{N} h_1(\varepsilon^{kk}_{\max}) \frac{K_m \rho_m}{\Delta\xi}\left(1 - e^{-\frac{\Delta\xi}{\rho_m}}\right)\right]\Delta\varepsilon_{kk} + \Delta\sigma^R_{kk} \tag{16}$$

and the residual part $\Delta\sigma^R_{kk}$ can be expressed in a recursive relation with the history variable S_m,

$$\Delta\sigma_{kk}^{R}=\sum_{m=1}^{M}-\left(1-e^{-\frac{\Delta\xi}{\rho_m}}\right)S_m(\xi_n),\text{and } S_m(\xi_n)=3K_m h_1\left(\varepsilon_{\max}^{kk}\right)R_{kk}\rho_m\left(1-e^{-\frac{\Delta\xi}{\rho_m}}\right)+S_m(\xi_{n-1})e^{-\frac{\Delta\xi}{\rho_m}} \tag{17}$$

For the deviatoric behavior, the formulation of the deviatoric behavior is obtained with constant deviatoric strain rate $\hat{R}_{ij}=\frac{\Delta\hat{\varepsilon}_{ij}}{\Delta\xi}$,

$$\Delta\hat{\sigma}_{ij}=2\left[G_\infty h_e\left(\varepsilon_{\max}^{e}\right)+\sum_{m=1}^{N}h_1\left(\varepsilon_{\max}^{e}\right)\frac{G_m\rho_m}{\Delta\xi}\left(1-e^{-\frac{\Delta\xi}{\rho_m}}\right)\right]\Delta\hat{\varepsilon}_{ij}+\Delta\hat{\sigma}_{ij}^{R} \tag{18}$$

where $\varepsilon_{\max}^{e}$ is the maximum equivalent strain, and the equivalent strain $\varepsilon_e=\sqrt{\frac{3}{2}\hat{\varepsilon}_{ij}\hat{\varepsilon}_{ij}}$. And the residual part $\Delta\hat{\sigma}_{ij}^{R}$ can be expressed in the recursive relation

$$\Delta\hat{\sigma}_{ij}^{R}=\sum_{m=1}^{N}-\left(1-e^{-\frac{\Delta\xi}{\rho_m}}\right)S_m(\xi_n),\text{and } S_m(\xi_n)=2G_m h_1\left(\varepsilon_{\max}^{e}\right)\hat{R}_{ij}\rho_m\left(1-e^{-\frac{\Delta\xi}{\rho_m}}\right)+S_m(\xi_{n-1})e^{-\frac{\Delta\xi}{\rho_m}} \tag{19}$$

Similarly, the incremental stress components can be developed from volumetric and deviatoric behaviors. The incremental 3D damage-coupled viscoelastic behavior can be formulated as

$$\begin{bmatrix}\Delta\sigma_{xx}\\ \Delta\sigma_{yy}\\ \Delta\sigma_{zz}\\ \Delta\sigma_{xy}\\ \Delta\sigma_{yz}\\ \Delta\sigma_{xz}\end{bmatrix}=\begin{bmatrix}K_{d1}&K_{d2}&K_{d2}&0&0&0\\ \cdot&K_{d1}&K_{d2}&0&0&0\\ \cdot&\cdot&K_{d1}&0&0&0\\ \cdot&\cdot&\cdot&K_{d3}&0&0\\ \cdot&\cdot&\cdot&\cdot&K_{d3}&0\\ \cdot&\cdot&\cdot&\cdot&\cdot&K_{d3}\end{bmatrix}\begin{bmatrix}\Delta\varepsilon_{xx}\\ \Delta\varepsilon_{yy}\\ \Delta\varepsilon_{zz}\\ \Delta\varepsilon_{xy}\\ \Delta\varepsilon_{yz}\\ \Delta\varepsilon_{xz}\end{bmatrix}+\begin{bmatrix}\Delta\sigma_{kk}^{R}+\Delta\hat{\sigma}_{xx}^{R}\\ \Delta\sigma_{kk}^{R}+\Delta\hat{\sigma}_{yy}^{R}\\ \Delta\sigma_{kk}^{R}+\Delta\hat{\sigma}_{zz}^{R}\\ \Delta\hat{\sigma}_{xy}^{R}\\ \Delta\hat{\sigma}_{yz}^{R}\\ \Delta\hat{\sigma}_{zx}^{R}\end{bmatrix} \tag{20}$$

With these terms:

$$\begin{aligned}\frac{\partial\Delta\sigma_{xx}}{\partial\Delta\varepsilon_{xx}}&=\left[K_\infty h_e\left(\varepsilon_{\max}^{e}\right)+\sum_{m=1}^{N}h_1\left(\varepsilon_{\max}^{e}\right)\frac{K_m\rho_m}{\Delta\xi}\left(1-e^{-\frac{\Delta\xi}{\rho_m}}\right)\right]\\&\quad+\frac{4}{3}\left[G_\infty h_e\left(\varepsilon_{\max}^{e}\right)+\sum_{m=1}^{N}h_1\left(\varepsilon_{\max}^{e}\right)\frac{G_m\rho_m}{\Delta\xi}\left(1-e^{-\frac{\Delta\xi}{\rho_m}}\right)\right]=K_{d1}\\ \frac{\partial\Delta\sigma_{xx}}{\partial\Delta\varepsilon_{yy}}&=\left[K_\infty h_e\left(\varepsilon_{\max}^{e}\right)+\sum_{m=1}^{N}h_1\left(\varepsilon_{\max}^{e}\right)\frac{K_m\rho_m}{\Delta\xi}\left(1-e^{-\frac{\Delta\xi}{\rho_m}}\right)\right]\\&\quad-\frac{2}{3}\left[G_\infty h_e\left(\varepsilon_{\max}^{e}\right)+\sum_{m=1}^{N}h_1\left(\varepsilon_{\max}^{e}\right)\frac{G_m\rho_m}{\Delta\xi}\left(1-e^{-\frac{\Delta\xi}{\rho_m}}\right)\right]=K_{d2}\\ \frac{\partial\Delta\sigma_{xy}}{\partial\Delta\varepsilon_{xy}}&=2\left[G_\infty h_e\left(\varepsilon_{\max}^{e}\right)+\sum_{m=1}^{N}h_1\left(\varepsilon_{\max}^{e}\right)\frac{G_m\rho_m}{\Delta\xi}\left(1-e^{-\frac{\Delta\xi}{\rho_m}}\right)\right]=K_{d3}\end{aligned} \tag{21}$$

The linear and damage-coupled viscoelastic models were defined in the ABAQUS user material subroutines for mastic subdomains. A displacement-based time-dependent finite element analysis was conducted by integrating elastic aggregate and linear and damage-coupled viscoelastic mastic to predict the global behavior of asphalt mixture.

Micromechanical Finite Element Simulation of Reclaimed Asphalt Mixture

As mentioned previously, reclaimed asphalt materials (similar as the regular hot mix asphalt) composed of very irregular aggregates and complex distributed mastic. The microstructures were divided into different aggregate and mastic subdomains. The finite element mesh was generated within the subdomains (aggregates and mastic) and along the subdomain boundaries. Fig. 1 shows the finite element meshes in the aggregates and mastic subdomains of a specimen surface. Finite elements in the neighboring subdomains share the nodes on irregular boundaries, and therefore the displacements of neighboring subdomains were connected through the shared nodes.

After the FE model has been developed, uniaxial compression test was simulated. For the compression simulation, the x- and y- displacements of the nodes on the bottom layer and the x- displacements of the nodes on the top layer were constrained. The sinusoidal cyclic force loading was evenly divided and imposed on nodes of the top layer. The evaluated Maxwell model parameters for asphalt mastic and elastic modulus of aggregates were inputted for predicting global viscoelastic properties. In the simulation, axial strain was calculated by dividing the average vertical displacement of top particles with the initial height of the undeformed specimen, and axial stress was obtained by dividing the constant loading force on the top layer with the specimen initial cross-section area.

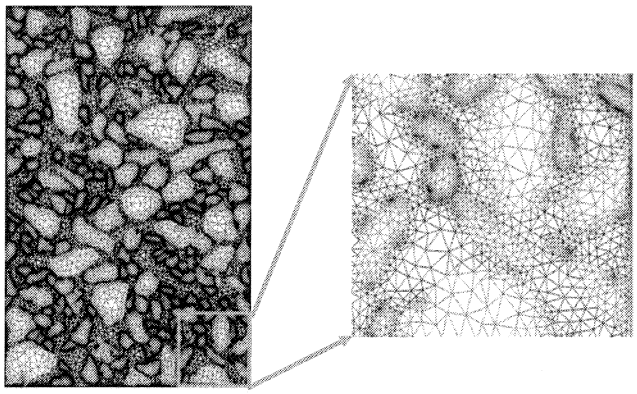

Fig. 1. The FEM meshes for the aggregate and mastic subdomains

Cyclic loading Simulation and Results

Sinusoidal cyclic force loading was imposed to the computational specimen to conduct uniaxial compression simulation under the different frequencies (0.1 Hz, 1 Hz, 5 Hz and 10 Hz). The laboratory tests of elastic aggregate (rock) and linear viscoelastic mastic were conducted to provide material input parameters for the FE models. The aggregate modulus takes a typical modulus of 55.5GPa for the limestone. The evaluate Maxwell model for reclaimed asphalt mastic includes one spring and four Maxwell elements in parallel ($E_\infty = 59.7MPa$, $E_1 = 5710.6MPa$, $\tau_1 = 26.2s$, $E_2 = 2075.1MPa$,

$\tau_2 = 311.9s$, $E_3 = 1449MPa$, $\tau_3 = 1678.8s$, $E_4 = 734.9MPa$, $\tau_1 = 19952.6s$). Model damage parameters were chosen as b=1, $\beta = 0.3$, and softening strain ε_0= 0.2 for the simulation.

Fig. 2 shows the cyclic simulation under the frequency of 0.1 Hz. The simulation was conducted with elastic aggregate and linear/damage-coupled viscoelastic mastic properties. In the figures, the black curve is the imposed compression stress loading with left-hand axial scales, and the magenta color indicates the strain response with right-hand axial scales. For better illustration, the final several cycles were magnified in the right-side figures for each frequency. The figures show the increasing creep compression strain along the loading time for the constant force loading magnitude. Comparing results (a) and (b) using linear and damage-coupled viscoelastic mastic properties, it shows viscoelastic damage behavior increases the sample creep deformation under the constant cyclic force loading. From the results of different loading frequencies, it was found that the uniaxial compression strain responses decease with the loading frequencies due to the less relaxation time. An ongoing experimental test plan will be conducted to verify the simulation results.

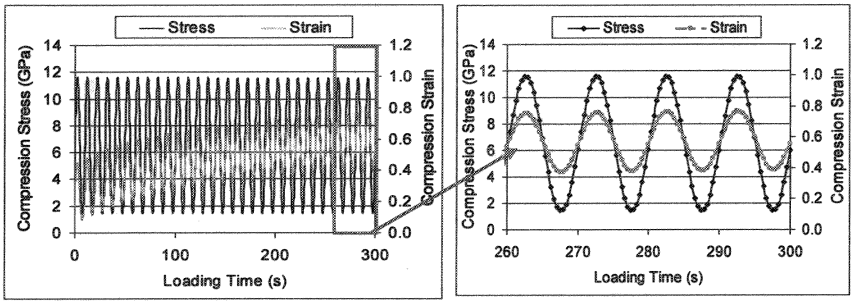

(a) Linear viscoelastic mastic

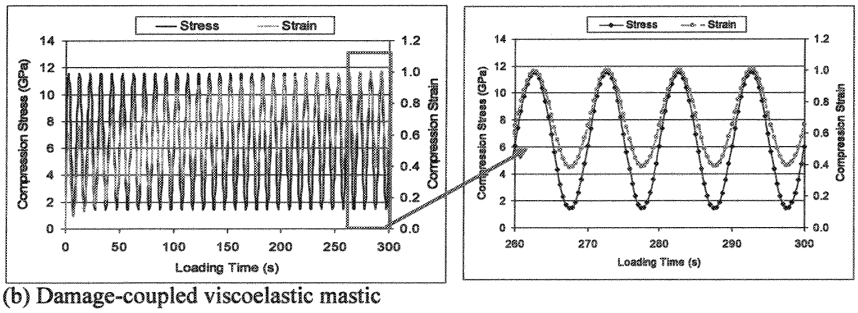

(b) Damage-coupled viscoelastic mastic

Fig. 2. The FEM simulation results under sinusoidal loading at a frequency of 0.1Hz

Summaries and Conclusions

The micromechanical Finite Element (FE) model by incorporating elastic aggregates and linear/damage-coupled viscoelastic mastic has been used to simulate viscoelastic behavior of a sustainable asphalt mixture -reclaimed asphalt mixture. The 2D microstructure of reclaimed asphalt mixture was obtained by optically scanning the smoothly sawn surface of asphalt specimens. In the microstructure, aggregates and sand mastic were divided into different subdomains. Finite element mesh was generated within each aggregate and sand mastic subdomain. Then the linear/damage-coupled viscoelastic mastic with specified properties defined in an ABAQUS user subroutine was combined with elastic aggregates to simulate global linear and damage-coupled viscoelastic behavior of reclaimed asphalt mixtures. Simulation results under a loading frequency showed the viscoelastic creep behavior under the constant loading magnitude. The damage-coupled viscoelastic mixture generated larger creep deformation comparing the linear behavior. Comparison under different loading frequencies found the compression strain decreases with frequencies due to less relaxation time. Simulation results indicate the developed finite element models are capable for complex viscoelastic behavior of reclaimed asphalt mixture. Further study will be extended to the three-dimensional micromechanical simulation.

References

Bahia, H., Zhai, H., Bonnetti, K., and Kose, S. (1999). "Nonlinear viscoelastic and fatigue properties of asphalt binders." *J. Assoc. Asphalt Paving Tech.*, 68, 1-34.

Bazant, Z. P., Tabbara, M.R., Kazemi, Y., Pijaudier-Cabot, G. (1990). " Random particle simulation of damage and fracture in particulate or fiber-reinforced composites. ." Damage Mechanics in Engineering Materials, Trans. ASME, AMD.

Budhu, M. S., Ramakrishnan, and Frantziskonis, G. "Modeling of Granular Materials: A Numerical Model Using Lattices, Mechanics of Deformation and Flow of Particulate Materials." *McNu Conference,Trans. ASCE*, Northwestern Univ.

Buttlar, W. G., Bozkurt, D., Al-Khateeb, G. G., and Waldhoff, A. S. (1999). *Understanding asphalt mastic behavior through micromechanics (with discussion and closure)*, Transportation Research Board.

Buttlar, W. G., and Roque, R. "Evaluation of empirical and theoretical models to determine asphalt mixture stiffnesses at low temperatures." Baltimore, MD, USA, 99-141.

Buttlar, W. G., and Roque, R. (1997). *Effect of asphalt mixture master compliance modeling technique on thermal cracking performance evaluation using superpave*, University of Washington, Seattle.

Buttlar, W. G., and You, Z. (2001). "Discrete Element Modeling of Asphalt Concrete: A Micro-Fabric Approach." *Journal of the Transportation Board, National Research Council, Washington, D.C.*, 1757.

Christensen, R. M., and Lo, K. H. (1979). "Solutions for Effective Shear Properties in Three Phase Sphere and Cylinder Models." *J. Mech. Phys. Solids*, 27, 315-330.

Dai, Q. (2004). "Micromechanical Modeling of Constitutive and Damage Behavior of Heterogeneous Asphalt Materials," University of Rhode Island.

Dai, Q., and Sadd, M. H. (2004). "Parametric model study of microstructure effects on damage behavior of asphalt samples." *International Journal of Pavement Engineering*, 5(1), 19-30.

Dai, Q., Sadd, M. H., and Parameswaran V. Shukla A. (2005). "Prediction of damage behaviors in asphalt materials using a micromechanical finite-element model and image analysis." *Journal of Engineering Mechanics*, 131(7), 668-677.

Dai, Q., Sadd, M. H., and You, Z. (2006). "A Micromechanical Finite Element Model for Viscoelastic Creep and Viscoelastic Damage Behavior of Asphalt Mixture." *International Journal for Numerical and Analytical Methods in Geomechanics*, 30, 1135–1158.

Dai, Q. and You, Z (2007), Prediction of Creep Stiffness of Asphalt Mixture with Micromechanical Finite Element and Discrete Element Models, Journal of Engineering Mechanics, American Society of Civil Engineers (ASCE), Volume 133, Issue 2, pp. 163-173.

Guddati, M. N., Feng, Z., and Kim, R. (2002). "Toward a micromechanics-based procedure to characterize fatigue performance of asphalt concrete." *Transportation Research Record*(1789), 121-128.

Hashin, Z. (1965). "Viscoelastic Behaviour of Heterogeneous Media." *In Journal of Applied Mechanics, Trans. ASME,*, 9, 630-636.

Hashin, Z., and Shtrikman, S. (1963). "A Variational Approach to the Theory of the Elastic Behaviour of Multiphase Materials." *J. Mech. Phys. Solids*, Vol. 11, 137.

Kose, S., Guler, M., Bahia, H. U., and Masad, E. (2000). "Distribution of Strains within Asphalt Binders in HMA Using Image and Finite Element Techniques." *J. Trans. Res. Record National Research Council, Washington, D.C.*, 1728(21-27).

McDaniel, R. S., and Shah, A. (2003). *Use of reclaimed asphalt pavement (rap) under superpave specifications (with discussion)*, Association of Asphalt Paving Technologists.

Mora, P. "A Lattice Solid Model for Rock Rheology and Tectonics." *The Seismic Simulation Project Tech.*, Institut de Physique du Globe, Paris, 3-28.

Mustoe, G. G. W., and Griffiths, D. V. "An Equivalent Model Using Discrete Element Method(DEM), ." *Proc. 12th ASCE Engineering Mechanics Conf.*, La Jolla, CA.

Papagiannakis, A. T., Abbas, A., and Masad, E. (2002). "Micromechanical analysis of viscoelastic properties of asphalt concretes." *Transportation Research Record*(1789), 113-120.

Picado-Santos, L. G., Oliveira, J. R. M., and Pereira, P. A. A. (2004). "Mechanical Characterisation of Hot Mix Recycled Materials." *International Journal of Pavement Engineering*, 5(4), pp 211-220.

Roberts, F. L., Kandhal, P. S., Brown, E. R., Lee, D. Y., and Kennedy, T. W. (1996). "Hot Mix Asphalt Materials, Mixture Design and Construction. Second Edition." NAPA Research and Education Foundation, 603 p.

Sadd, M. H., Dai, Q., and Parameswaran, V. (2004a). "Microstructural simulation of asphalt materials: Modeling and experimental studies." *Journal of Materials in Civil Engineering*, 16(2), 107-115.

Sadd, M. H., Dai, Q., Parameswaran, V., and Shukla, A. (2004b). "Microstructural simulation of asphalt materials: Modeling and experimental studies." *Journal of Materials in Civil Engineering*, 16(2), 107-115.

Sadd, M. H., Dai, Q., Parameswaran, V., and Shukla, A. (2004c). "Simulation of Asphalt Materials Using Finite Element Micromechanical Model with Damage Mechanics." *Transportation Research Record*(1832), 86-95.

Schapery, R. A. (1969). "On the characterization of nonlinear viscoelastic materials." *Polymer Engineering and Science*, 9(4), 295-310.

Sepehr, K., Svec, O. J., Yue, Z. Q., and El Hussein, H. M. "Finite element modelling of asphalt concrete microstructure." Udine, Italy, 225.

Shashidhar, N., Needham, S. P., Chollar, B. H., and Romero, P. (1996). "Prediction of the performance of mineral fillers in stone matrix asphalt." *J. Assoc. Asphalt Paving Tech.*, 222-251.

Simo, J. C., and Ju, J. W. (1987). "Strain- and Stress-Based Continuum Damage Models - I. Formulation." *International Journal of Solids and Structures*, 23(7), 821-840.

Stankowski , T. (1990). "Numerical Simulation of Failure in Particle Composite, Computers and Structures." *Computers and Structures, Great Britain*, 44(1/2), 460.

Voigt, W. (1889). *Ueber die Beziehung zwischen den beiden Elasticitatsconstanten isotroper Korper*.

You, Z. (2003). "Development of a Micromechanical Modeling Approach to Predict Asphalt Mixture Stiffness Using Discrete Element Method," University of Illinois at Urbana-Champaign, published by UMI, a Bell & Howell Information Company, Ann Arbor, MI.

You, Z., and Buttlar, W. G. (2004). "Discrete Element Modeling to Predict the Modulus of Asphalt Concrete Mixtures." *Journal of Materials in Civil Engineering, ASCE*, 16(2), 140-146.

You, Z., and Buttlar, W. G. (2005). "Application of Discrete Element Modeling Techniques to Predict the Complex Modulus of Asphalt–Aggregate Hollow Cylinders Subjected to Internal Pressure." *Journal of the Transportation Research Board, National Research Council*, 1929, 218-226.

You, Z., and Buttlar, W. G. (2006). "Micromechanical Modeling Approach to Predict Compressive Dynamic Moduli of Asphalt Mixture Using the Distinct Element Method." *Journal of the Transportation Research Board, National Research Council, Washington, D.C.*, No. 1970, 73-83.

